Ice Nucleation by Alcohols Arranged in Monolayers at the Surface of Water Drops

MICHAL GAVISH, RONIT POPOVITZ-BIRO, MEIR LAHAV,
LESLIE LEISEROWITZ

Monolayers of aliphatic long-chain alcohols induced nucleation of ice at temperatures approaching 0°C, in contrast with water-soluble alcohols, which are effective antifreeze agents. The corresponding fatty acids, or alcohols with bulky hydrophobic groups, induce freezing at temperatures as much as 12°C lower. The freezing point induced by the amphiphilic alcohols was sensitive not only to surface area per molecule but, for the aliphatic series ($C_nH_{2n+1}OH$), to chain length and parity. The freezing point for chains with *n* odd reached an asymptotic temperature of 0°C for an upper value of $n = 31$; for *n* even the freezing point reached a plateau of −8°C for *n* in the upper range of 22 to 30. The higher freezing point induced by the aliphatic alcohols is due to formation of ordered clusters in the uncompressed state as detected by grazing incidence synchrotron x-ray diffraction measurements. The diffraction data indicate a close lattice match with the *ab* layer of hexagonal ice.

PURE WATER CAN BE SUPERCOOLED to temperatures of −20° to −40°C. Therefore the induction or inhibition of freezing of ice, in particular through the role of auxiliaries such as membranes or proteins, has far-reaching ramifications for the living and the nonliving world. Promotion of ice nucleation has been exploited in the induced precipitation of rain by silver iodide seeded in clouds (*1, 2*). On the other hand, it can result in wide scale damage to crops by frost bacteria (*3, 4*), which nucleate ice at −4°C. An intriguing example of inhibition involves the activity of antifreeze proteins in the blood serum of fish in polar seas; these proteins lower the freezing point by no more than 2°C, but this small difference is vital for their survival (*5*).

Ice nucleation has been widely studied, yet the role played by auxiliaries involved in the promotion of ice nucleation is still obscure. Several mechanisms have been proposed, such as a lattice or structural match between the substrate and the nucleated ice crystal (*6*) or an electric field present in the substrate that orients the water molecules to induce ice nucleation (*7*). In order to unravel the complexity of this process, we designed experiments where two such mechanisms can be studied independently. We focus on the first effect and present the use of Langmuir monolayers for induced ice nucleation.

Both compressed or uncompressed monolayers of amphiphiles can promote oriented crystal growth at the monolayer-solution interface. This induction was achieved by a structural fit or complementarity between the attached face of the nucleated crystal and the hydrophilic head groups of the monolayer (*8, 9*), the structure of which was independently determined by grazing-incidence x-ray diffraction (GIXD) (*10*). The extent of oriented crystallization could be varied by using amphiphiles with different cross-sectional areas and thus change the degree of fit between the monolayer and the nucleated crystal.

The stable form of ice (Fig. 1) crystallized under atmospheric pressure is hexagonal, space group $P6_3/mmc$, with axes $a = b = 4.5$, $c = 7.3$ Å, $\gamma = 120°$ at −50°C (*11*). The crystal structure may be described, in terms of the O atoms, as composed of 0.9 Å thick bilayers parallel to the *ab* plane separated by 2.75 Å along the *c* axis. Each O atom participates in three O−H···O hydrogen bonds within the bilayer and a fourth O−H···O bond of 2.75 Å interlinking the neighboring close-packed bilayers. The area per water molecule within a layer is $a^2 \sin 120° = 17.5$ Å^2.

The crystalline structure of the compressed monolayer of the alcohol $C_{21}H_{43}OH$ on water has recently been characterized by GIXD by Dutta, Rice, and co-workers (*12*). The unit cell of the crystalline monolayer at temperatures just above 0°C is distorted hexagonal, (Fig. 2A) with axes $a = b = 4.5$ Å, $\gamma = 113°$, and area per molecule $a^2 \sin \gamma = 18.6$ Å^2. It may be more properly characterized as centered rectangular, $a' = 7.42$ Å and $b' = 5.00$ Å. The molecular chain of $C_{21}H_{43}OH$ appears to be slightly tilted with respect to the normal to the water surface. Thus the arrangement of its OH head groups at the water surface would appear to mimic or complement a hexagonal layer of ice. The proposed structural match between the monolayer and a layer of ice in the *ab* plane suggested that such monolayers should be efficient nucleators of ice (Fig. 2B).

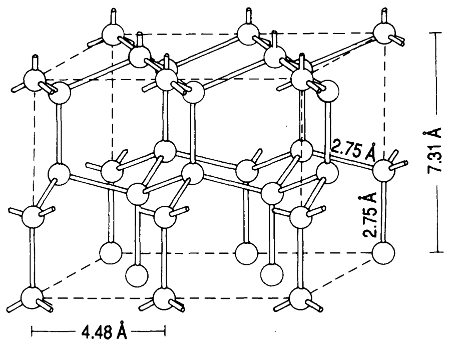

Fig. 1. Crystal structure of hexagonal ice. The oxygen atoms of each water molecule are denoted by a ball and the disordered O−H···O hydrogen bonds by rods. The hexagonal *a* and *c* axes are specified.

The freezing point measurements were carried out on two water drops of the same size (ranging from 10 to 40 μl) placed on a cooling stage in a box purged by cooled nitrogen gas. One drop was completely covered with a monolayer of the amphiphilic chain alcohol and the other with a reference material (*13*). As reference we used the corresponding long-chain fatty acid or the alcohol $C_{31}H_{63}OH$. In this way the effect of factors responsible for induction of nucleation, other than a difference in structural match, were eliminated.

The freezing point measurements (Fig. 3) showed that aliphatic chain alcohols nucleate ice at higher temperatures, and with greater reproducibility than the analogous carboxylic acids. The freezing point of drops of pure water, by way of comparison, ranged from −20° to −25°C.

It is striking that the freezing point is sensitive to the length and parity of the chain of $C^{n}H_{2n+1}OH$. The freezing point curve for the *n*-odd series increases asymptotically with chain length, approaching 0°C for $n = 31$. The *n*-even series behaves differently; the freezing point curve reaches a plateau of about −8°C for *n* in the range of 22 to 30. This trend suggests that just prior to ice nucleation, the orientation of the OH groups in the odd and even analogs are not the same, the former having a structural fit closer to the *ab* layer of ice (*14*).

We recently performed GIXD measurements on the liquid surface diffractormeter at the synchrotron beamline D4 at Hasylab on monolayers of $C_{23}H_{47}OH$, $C_{30}H_{61}OH$, $C_{31}H_{63}OH$, and $C_{29}H_{59}CO_2H$ over pure water at 5°C (*15*). The measurements were made on monolayers in an uncompressed state at approximately 70% surface coverage. Diffraction peaks were observed for all four monolayers yielding coherence lengths (that is, the crystalline domain size) in the range of 300 to 1000 Å that indicated pronounced crystalline self-aggregation

---

Department of Structural Chemistry, The Weizmann Institute of Science, Rehovot 76100, Israel.

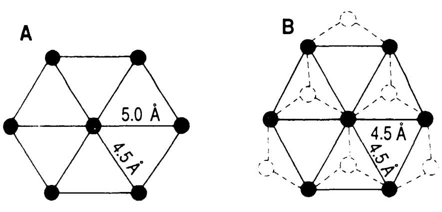

Fig. 2. (**A**) Distorted hexagonal lattice of a compressed aliphatic alcohol monolayer on water. (**B**) The lattice of hexagonal ice as viewed along the *c* axis. The oxygen atoms of two layers separated by 0.9 Å are depicted as one full and one dotted.

(*15*). The diffraction spectrum of $C_{31}H_{63}OH$ is shown in Fig. 4. The unit cells of the uncompressed monolayers are given in Table 1. There is a good fit between the *ab* lattice of hexagonal ice and the *ab* lattices of three alcohols but not with that of the acid monolayer, in keeping with the freezing point measurements. We note the minor differences in cell dimensions of the C_{30} (*n*-even) and C_{31} (*n*-odd) monolayers. The intensity distribution of their Bragg rod diffraction data, which shall be analyzed elsewhere (*15*), indicates a difference in chain tilt angle of about 3° with an average value of about 10° from the normal water surface. Whether there is a closer match of the monolayer lattice to that of ice at the freezing point must await further GIXD measurements.

The effect of increasing the cross-sectional area of the alcohol was also monitored. Introduction of an amide function in the chain to form the alcohol $C_{11}H_{23}CONH\text{-}C_{11}H_{22}OH$ imposes a minor increase in molecular area from 20 to 24 Å² together with an increase in length of one of the axes from 4.5 to 4.9 Å to enable N−H···O (amide) hydrogen bonding. This amphiphile induces freezing at about −12°C, distinctly lower than that of the aliphatic alcohol of a similar length, as expected. Perfluorododecanol and cholesterol, which have molecular areas (28 and 38 Å², respectively) that are decidely greater than the *ab* unit cell area of ice (17.5 Å²), were poor ice nucleators.

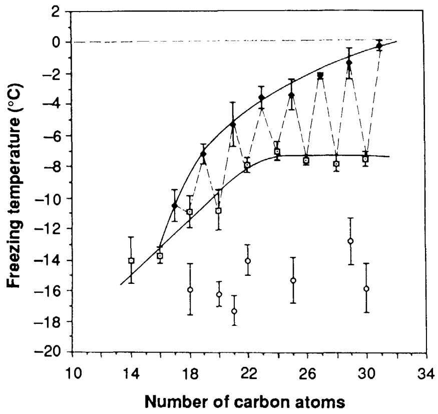

Fig. 3. Freezing points of drops of supercooled water covered by monolayers of alcohols $C^nH_{2n+1}OH$ (*n* even, ⊡ and *n* odd, ●) and carboxylic acids $C^nH_{2n+1}CO_2H$ (○). Freezing point curves are drawn separately for alcohols with *n* odd and *n* even. The error bars (±SD) for each point were derived from 10 to 20 freezing point measurements. All materials, except for alcohols *n* = 23, 29, and 31 were purchased from Sigma and were specified 98 to 99% pure by capillary gas chromatography. The alcohols *n* = *23*, *29*, and 31 were synthesized by reducing the corresponding methyl esters with $LiAlH_4$ and purified by column chromatography on silica gel using CH_2Cl_2 as eluent.

Table 1. Cell constants (unit cell dimensions *a* and *b* and the angle γ, where the area is *ab* sinγ) of uncompressed monolayers over pure water at 5°C.

Monolayer	*a* = *b* (Å)	γ (degrees)	*ab* sin-γ (Å²)
$C_{23}H_{47}OH$	4.54	113.0	19.0
$C_{30}H_{61}OH$	4.50	112.8	18.7
$C_{31}H_{63}OH$	4.52	113.1	18.8
$C_{29}H_{59}CO_2H$	4.65	106.3	20.7

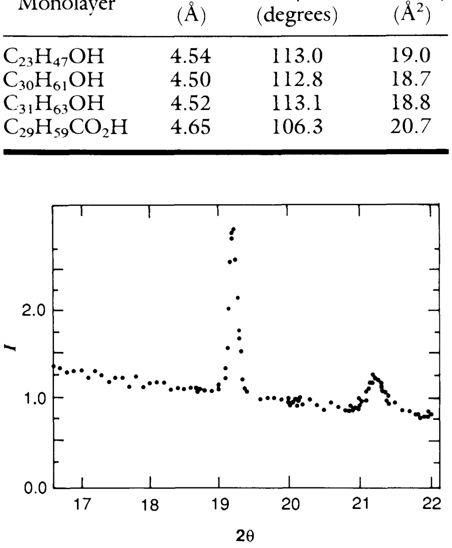

Fig. 4. Part of a GIXD spectrum of an uncompressed monolayer of $C_{31}H_{63}OH$ over pure water at 5°C with a wavelength of 1.3875 Å (*15*).

The effect on the freezing point by the extent of monolayer coverage on the water drop was also examined. A series of measurements for $C_{30}H_{61}OH$ shows that for coverage of 75% the nucleation temperature fell by 2°C, as compared to 100% coverage. For 50% coverage there was a drop in freezing point by about 8°C. In another set of measurements the monolayers were prepared from mixed amphiphilic solutions composed of $C_{20}H_{41}OH$ and $C_{12}F_{21}H_4OH$. The pressure-area isotherms of this mixture showed that it does not form a solid solution but segregates into two phases. The freezing point stayed the same for mixtures with a molar fraction of the hydrocarbon alcohol down to ~75%. Below this value till ~25% the freezing point dropped by about 2°C. The first set of experiments suggest a reduced crystallinity of the monolayer due to incomplete coverage (*16*), whereas the second set of results indicates that the hydrocarbon alcohol forms well-ordered crystalline clusters amidst a sea of fluorocarbon molecules (*17*).

This study demonstrates that alcohols may act not only as antifreeze agents when present in solution but, when constrained to the water surface, form self-assembled clusters that are highly efficient ice nucleators by virtue of a structural fit with that of ice. This type of dichotomy has been observed previously for α-amino acids (*8*) and proteins involved in biomineralization (*18*). The relatively high freezing point of pure water induced by some of the alcohols opens possibilities for the design of efficient auxiliaries for cloud seeding. The results obtained also suggest that induced ice nucleation in biological systems such as frost bacteria (*2*, *4*, *19*) may involve a structural match or a deviation therefrom, but does not exclude other types of freezing mechanisms.

REFERENCES AND NOTES

1. B. Vonnegut, *J. Appl. Phys.* **18**, 593 (1947).
2. M. L. Corrin and J. A. Nelson, *J. Phys. Chem.* **72**, 643 (1968).
3. R. C. Schnell and C. Vali, *Nature* **263**, 163 (1972); S. E. Lindow, D. C. Arny, C. D. Upper, *Phytopathology* **68**, 523 (1978).
4. L. R. Maki, E. L. Galyon, M. Chang Chien, D. R. Colwell, *Appl. Microbiol.* **28**, 456 (1974).
5. A. L. DeVries, *Philos. Trans. R. Soc. London Ser. B* **304**, 575 (1984); R. E. Feeney, T. S. Burcham, Y. Yeh, *Ann. Rev. Biophys. Biophys. Chem.* **15**, 59 (1986); D. S. C. Yang, M. Sax, A. Chakrabartty, C. L. Hew, *Nature* **333**, 232 (1988).
6. N. Y. Fletcher, *The Chemical Physics of Ice* (Cambridge Univ. Press, Cambridge, 1970), pp. 73–103.
7. H. R. Prappacher, *Z. Angew. Math. Phys.* **14**, 590 (1963).
8. E. M. Landau, M. Levanon, L. Leiserowitz, M. Lahav, J. Sagiv, *Nature* **318**, 353 (1985).
9. I. Weissbuch, G. Berkovic, L. Leiserowitz, M. Lahav, *J. Am. Chem. Soc.* **112**, 5874 (1990); E. M. Landau, R. Popovitz-Biro, M. Levanon, L. Leiserowitz, M. Lahav, *Mol. Cryst. Liq. Cryst.* **134**, 323 (1986); E. M. Landau *et al.*, *Pure Appl. Chem.* **6**, 673 (1989); E. M. Landau *et al.*, *J. Am. Chem. Soc.* **111**, 1436 (1989); S. Mann, B. Heywood, S. Rajam, J. D. Birchall, *Nature* **334**, 692 (1988).
10. D. Jacquemain *et al.*, *Colloq. Phys.* **50** (suppl. no. 10), C7-29 (1989).
11. L. Pauling, *J. Am. Chem. Soc.* **57**, 2680 (1935); S. W. Peterson and H. A. Levy, *Acta Cryst.* **10**, 70 (1957).
12. S. W. Barton *et al.*, *J. Chem. Phys.* **89**, 2257 (1988).
13. The temperature of the two drops was monitored simultaneously with a thermocouple. The thermocouple was calibrated at 0°C by measuring the melting point of ice in separate experiments. The water drops were cooled at a rate of 2°C min.
14. The effect of curvature of the water drops on the monolayer arrangement may be neglected because of the large volume of the water drops (10 to 40 μl) relative to the cross-sectional area of the amphiphile.
15. D. Jacquemain *et al.*, unpublished results.
16. This deduction is consistent with GIXD measurements from fatty acid $C_{19}H_{39}CO_2H$ monolayers on water, albeit at room temperature (*17*); the data indicated a pronounced reduction in crystalline order and coherence length (that is, perfect crystalline domain size) for low monolayer coverage.
17. The deduction is consistent with GIXD measurements from a monolayer on water comprising a mixture of an aliphatic alcohol and an amino acid with a fluorocarbon chain. The diffraction spectrum signaled the presence of crystalline clusters of the

former even though its concentration was as low as 10% (F. Leveiller, unpublished results).
18. L. Addadi and S. Weiner, *Proc. Natl. Acad. Sci. U.S.A.* **82**, 4110 (1985).
19. G. J. Warren, *Biotechnol. Genet. Eng. Rev.* **5**, 107 (1987); H. Mizuno, *Proteins* **5**, 47 (1989).
20. We thank E. Shavit and I. Müller for participation in the experiments. We acknowledge a preindustrial grant from Yeda and financial support from the U.S.–Israel Binational Foundation and the Petroleum Fund of the American Chemical Society. M.G. thanks the Feinberg Graduate School of the Weizmann Institute of Science for a postdoctoral fellowship.

31 May 1990; accepted 28 August 1990

Chiral Symmetry Breaking in Sodium Chlorate Crystallization

DILIP K. KONDEPUDI,* REBECCA J. KAUFMAN, NOLINI SINGH

Sodium chlorate ($NaClO_3$) crystals are optically active although the molecules of the compound are not chiral. When crystallized from an aqueous solution while the solution is not stirred, statistically equal numbers of levo (L) and dextro (D) $NaClO_3$ crystals were found. When the solution was stirred, however, almost all of the $NaClO_3$ crystals (99.7 percent) in a particular sample had the same chirality, either levo or dextro. This result represents an experimental demonstration of chiral symmetry breaking or total spontaneous resolution on a macroscopic level brought about by autocatalysis and competition between L- and D-crystals.

IN NATURE WE FIND STATES OF BROKEN chiral symmetry at all levels, from elementary particles to the biosphere (*1*). Processes that lead to transitions from a chirally symmetric state to a totally asymmetric state are thus of general interest. Although many mechanisms that produce totally asymmetric macroscopic states exist in theory (*2–4*), none have been experimentally realized. The difficulty has been that these models require both autocatalysis and competition between the left- and the right-handed products. Here we report how so simple a process as constant stirring of the solution generates both autocatalysis and competition and thus can produce totally asymmetric macroscopic states of crystals that all have the same handedness.

The nucleation of achiral $NaClO_3$ molecules to form an optically active chiral crystal is an example of symmetry breaking, but at a microscopic level. In a typical crystallization, however, the chiral symmetry is restored, in that statistically equal numbers of L- and D-crystals are obtained, as was shown by the experiments of Kipping and Pope almost 100 years ago (*5*).

More recently, Pincock *et al.* (*6–8*) performed a careful statistical study on 1,1′-binaphthyl. For the proportion of molecules that crystallized in one of the two enantiomeric forms, they obtained a distribution that is close to a Gaussian with a mean of 50%. These experiments clearly showed that the two enantiomorphs will be found in equal proportion; any deviation from chiral symmetry is a result of statistical fluctuation. As Pincock *et al.* note, "From this distribution it is apparent that obtaining binaphthyl with an optical purity above 90 percent by this method would be a very exceptional event (observable about one in 150 tries)" (*6*, p. 1019). In order to produce total asymmetry of close to 100% in the product crystals in every try, autocatalysis and competition between the L- and the D-crystals are needed.

We note that in crystallization experiments unequal numbers of L- and D-crystals are often encountered due to the presence of impurities (*9, 10*). On the other hand, numerous studies [see, for example, (*11–13*), and references therein] have investigated enantioselective crystallization induced by the presence of optically active compounds, seeds, or other asymmetric influences. In these cases, the predominance of one chirality is not due to an intrinsic mechanism of symmetry breaking and it does not occur spontaneously.

We first performed the crystallization without stirring and found results similar to those found by Kipping and Pope (*5*): in a total of 1000 crystals obtained from 17 different crystallizations, 525 were found to be levo and 475 were dextro. Of the 17 crystallizations, 8 produced slightly more L- than D-crystals because of statistical fluctuations.

The above crystallizations were performed as follows. A solution of $NaClO_3$ was prepared by dissolving ∼100 g of $NaClO_3$ (of 99.9% purity) in ∼120 ml of distilled water. The resulting solution was constantly stirred and heated to ∼50°C. The stirring was continued for ∼30 min to ensure complete desolution of the solute. The solution was then filtered and cooled to room temperature (∼25°C). Samples of ∼25 ml of this solution were transferred to several petri dishes and left for crystals to grow. The initial concentration was such that cooling alone did not produce any crystals; evaporation of the solution was necessary. Temperature was not controlled, and it varied about ±3°C. After 4 to 5 days, the crystals that were large and optically transparent enough for the detection of optical rotation were separated. The smallest of these crystals were ∼1 mm in size. We used a pair of polarizers to separate and count the L- and D-crystals. When white light is used, the crystals appear blue when the polarizers are crossed and turn red on rotating the analyzer clockwise or anticlockwise depending on the crystal's handedness. For a 1-mm crystal, the change in color from blue to red occurs for a rotation of about 7°.

We found that constant stirring of the solution has a dramatic effect on the enantiomorphic ratio of the $NaClO_3$ crystals: in each sample the crystals are almost all dextro- or all levo-rotatory. This process occurred without the need for careful control of temperature or other conditions.

Samples of the $NaClO_3$ solution (25 ml) prepared as described above were transferred to several 100-ml beakers and stirred constantly with a magnetic stirrer and a 12 mm by 4 mm by 4 mm Teflon stirbar. The beakers were covered with tissue paper to prevent dust particles from entering the system and to slow the rate of evaporation. All of the stirrer speeds were set at the same level (∼100 rpm). As before, L- and D-crystals were separated and counted. These crystals were in general smaller and more numerous than those found in unstirred experiments; they were also more rounded.

In a total of 32 different crystallizations, 18 were predominantly dextro while 14 were predominantly levo. No sample that produced crystals was discarded. In Table 1 the crystal counts are shown for each of the 32 crystallizations. Stirrers, with fixed direction of stirring, produced both L- and D-dominated crystallizations in different runs. A total of 11,829 crystals were counted. As can be seen from the data, amidst predominantly L-crystals a small number of D-crystals grew and vice versa. Similar asymmetric crystallization was also obtained when an overhead stirrer was used.

In the 18 D-dominated crystallizations in Table 1, the fraction of D-crystals is found to

Department of Chemistry, Box 7486, Wake Forest University, Winston-Salem, NC 27109.